JOURNAL OF THEORETICAL AND APPLIED MECHANICS
51, 3, pp. 553-567, Warsaw 2013

DEVELOPMENT OF A THERMAL MODEL IN THE METAL CUTTING PROCESS FOR PREDICTION OF TEMPERATURE DISTRIBUTIONS AT THE TOOL-CHIP-WORKPIECE INTERFACE

Abdelkader Karas, Mohamed Bouzit

Laboratory of Mechanics Applied, Faculty of Mechanical Engineering USTO-MB, Oran, Algeria

e-mail: karasaek@yahoo.fr; bouzit_mohamed@yahoo.fr

Mustapha Belarbi

Ibn-Khaldun University of Tiaret, Electrical Engineering Department, Algeria

e-mail: mustapha_belarbi@yahoo.fr

The prediction of temperature distributions in the tool-chip-workpiece interface is not obvious with the complexity of the induced phenomena. For this purpose, we developed a thermal model in orthogonal metal cutting based on the thermal model of Komanduri and Hou that determines temperature distributions in the tool-chip-workpiece separately, each in its own axes system. The overall distribution is obtained by assembling three temperature distributions at the tool-chip-workpiece interface. Our developed model returns global temperature distributions in the real time throughout the tool-chip-workpiece in the same coordinate system. Our simulation results compared to the original maps showed a perfect correspondence, unlike the computation time and computation steps.

Key word: orthogonal metal cutting, thermal modeling, moving heat source

Nomenclature

a	–	thermal diffusivity [cm^2/s]
$B, (1-B)$	–	fraction of shear plane heat conducted into workpiece and into chip, respectively
F_c, F_t, F_{fr}	–	cutting, thrust, frictional force at chip-tool interface, respectively [N]
l_i	–	location of differential small segment of shear band heat source dl_i relative to upper end along width [cm]
M	–	any point in medium with temperature rise concerned
L	–	width of shear band heat source
K_0	–	modified Bessel function of second kind and zero order
q_{pl}, q_{pli}, q_{pls}	–	heat liberation intensity of moving plane heat source, induced plane heat source and shear plane heat source, respectively [$\mathrm{J/cm^2 s}$]
R	–	distance between moving line heat source and point M [cm]
r_c	–	thickness ratio of chip
t_{ch}	–	depth of cut or thickness of undeformed chip [cm]
V, V_c, V_{ch}, V_s	–	velocity of moving plane heat source, cutting speed, chip and shear velocity, respectively [cm/s]
w	–	width of cut [cm]
X, z	–	coordinates of point M in moving coordinate system [cm]
T_M	–	temperature rise at point M [°C]
λ, λ_{tool}	–	thermal conductivity, thermal conductivity of tool, respectively [$\mathrm{J/cm\,s\,^\circ C}$]
τ	–	shear stress on shear plane [$\mathrm{N/cm^2}$]
α, ϕ, φ	–	rake, shear and oblique angle, respectively [deg]

1. Introduction

The modeling of machining temperatures has attracted many researchers because of the complexity of measuring temperatures during machining. Many analytical models have been proposed to predict temperature distributions in deformation zones. Pioneering studies were performed by Hahn (1951), Trigger and Chao (1951), Chao and Trigger (1953, 1955, 1958), Loewen and Shaw (1954), Leone (1954), Boothroyd (1963) and recently by Komanduri and Hou (2000, 2001a,b), Huang and Liang (2005), Karpat and Özel (2006-2008).

At the forefront of analytical modeling, based on the moving heat source method by Jaeger (1942) and Carslaw and Jaeger (1959), the analytical modeling of steady-state temperature in metal cutting was presented by Hahn (1951), Trigger and Chao (1951), Chao and Trigger (1958), Loewen and Shaw (1954), and more recently by Komanduri and Hou (2000, 2001a,b). The commonalties of these models are the consideration of heat sources at the primary and secondary shear zones with related boundary conditions and the assumption that the bulk of the deformation energy is converted into heat while a negligible amount is stored as latent energy in the deformed metal. However, there are differences in these models in the way the heat source properties and boundary conditions were treated.

In treating the primary heat source, the models are different in considering the nature, the moving direction, and the velocity of the heat source as well as in estimating the heat partition ratio and the boundary conditions. For example, when modeling the temperature rise on the chip side, the velocity of the moving heat source was treated differently as the chip velocity in the work by Hahn (1951), Komanduri and Hou (2000), as the cutting velocity in the work by Chao and Trigger (1953), and as the shear velocity in the work by Loewen and Shaw (1954). Furthermore, except for works by Hahn (1951), Chao and Trigger (1953), Komanduri and Hou (2000), most models considered the primary heat source as a result of two bodies in sliding contact and used Blok's (1938) heat partition approach for the evaluation of the average temperature within the primary shear zone. Realizing the fact that there is actually only one body involved in the primary shear zone, Komanduri and Hou (2000) proposed that the temperature rise on the chip due to the primary heat source should be the effect of an oblique band heat source moving at chip velocity within a semi-infinite medium. They also argued that the temperature rise on the workpiece is a result of an oblique band heat source moving at the cutting velocity within a semi-infinite medium. No boundary along the tool-chip interface was considered when modeling the effect of the primary heat source, though an insulated boundary condition along the tool-chip interface was used when modeling the effect of the secondary heat source. In evaluating the combined effects of two heat sources, Komanduri and Hou (2001b) considered the effect of the primary heat source on the final temperature rise within the tool by introducing an induced stationary rectangular heat source caused by the primary heat source.

When modeling the effect of the secondary heat source, the heat partition approach is commonly applied by considering a pair contact of the tool and the chip. Chao and Trigger (1955) used Blok's (1938) partition principle by assuming a uniform heat partition ratio along the tool-chip contact length, but failed to achieve a temperature rise on the chip in agreement with that on the tool along the interface. To resolve this issue, Chao and Trigger (1955) suggested that there was a non-uniform distribution of the heat partition ratio along the contact length and tried a functional analysis method, discrete numerical iterative method, and a method in which the linear algebraic equations (Chao and Trigger, 1958) are simultaneously solved. On the other hand, Chao and Trigger (1958) simply assumed that the heat intensities along the tool-chip and tool-workpiece interfaces were uniform, which actually should be a combination of plastic and elastic zones with different heat intensities, respectively. Recently, Komanduri and Hou (2001a) furthered the functional analysis approach based on the idea of Chao and Trigger (1955), but no perfect function has been found. Although those studies by Chao and Trigger

(1958), Komanduri and Hou (2001a) have adopted the concept of a non-uniform distribution of the heat partition ratio, they all treated the heat intensity along the tool-chip interface as uniform. Wright *et al.* (1980) modeled the effect of the secondary heat source by applying a non-uniform heat intensity, but applied a uniform heat partition ratio which was determined empirically. Until now, there is no documented model that considers both the non-uniform heat partition ratio and non-uniform heat intensity along the tool-chip interface.

Komanduri and Hou (2001b) combined the thermal effects associated with the heat sources at the primary and the secondary shear zones to predict temperature in the tool-chip-workpiece interface. The temperature map obtained is in fact only one superposition of various temperature maps obtained each time in its own coordinate system.

This work is an improvement of Komanduri and Hou's thermal model; therefore we proceed to rewrite the equations which express the temperature of the chip, the tool and the workpiece in the same system of axes. For this purpose, the system of axes retained is that of the workpiece; the mathematical transformations (translation and rotation) are brought thereafter.

2. Thermal modeling of Komanduri and Hou's model

2.1. Primary shear zone

Komanduri and Hou's works (2000) on the study of heat transfer in the primary shear zone were inspired by the developments of Hahn (1951). Hahn used the results of Jaeger (1942) and Rosenthal (1946) concerning the moving band heat source and proposed an original and realistic modeling of thermal phenomenon in the primary shear zone. Indeed, he considered the workpiece and the chip as only one body (an infinite medium) in which moves a linear heat source obliquely. Figure 1 shows modifications brought by Komanduri and Hou.

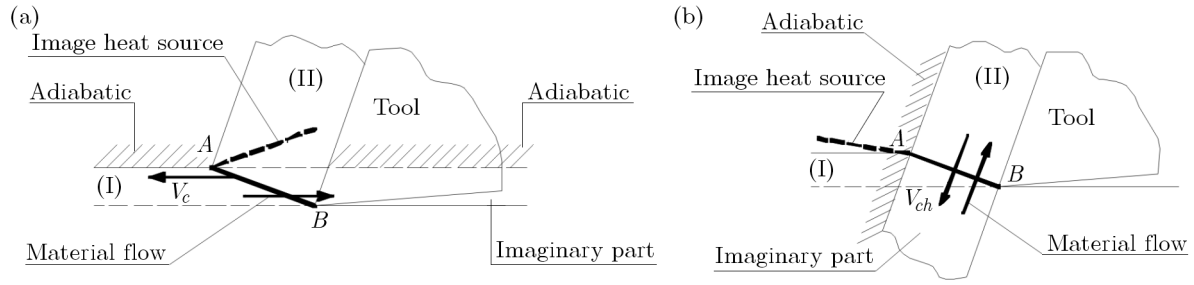

Fig. 1. Assumptions of Komanduri and Hou's model; (a) model for thermal analysis of the work piece, (b) model for thermal analysis of the chip

In the case of dry machining, they consider that the primary shear zone can be compared to a band of heat of width L and infinite length. This band moves in a semi-infinite medium parallel to its border (border of the medium), tilted by an angle φ to its limit, and one of its edges is on the adiabatic border of the medium. This latter represents the workpiece and the chip; the adiabatic border being the surface of the workpiece and the chip which is in contact with the ambient air. Figure 2 shows a scheme the concept of the oblique moving band heat source.

Let us note that the temperature in a point M of the medium due to the oblique moving heat source of an infinite extension and intensity q_{pl} moving at the speed V in an infinite medium is expressed in the following way

$$T_M = \frac{q_{pl}}{2\pi\lambda} \int_{l_i=0}^{L} \exp\Big(-(X - l_i \sin\varphi)\frac{V}{2a}\Big) K_0\Big(\frac{V}{2a}\sqrt{(X - l_i \sin\varphi)^2 + (z - l_i \cos\varphi)^2}\Big)\, dl_i \qquad (2.1)$$

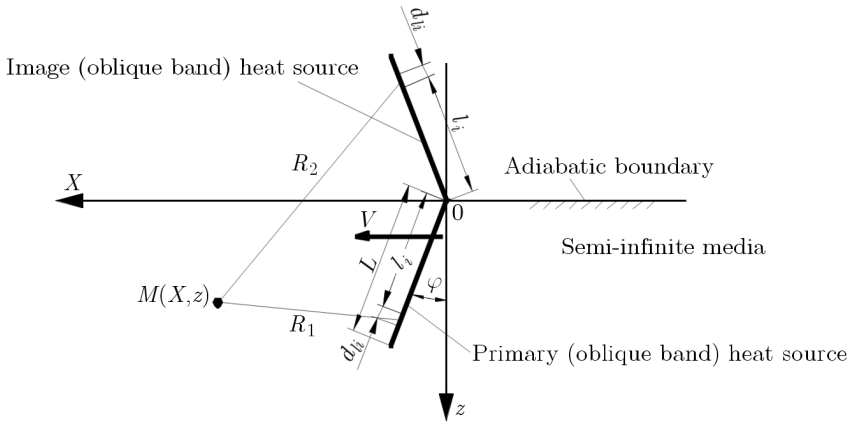

Fig. 2. Oblique moving band heat source in an infinite medium

To reconsider the semi-infinite nature of the medium, Komanduri and Hou take into account the contribution of a symmetrical imaginary heat source of the first one in relation to the adiabatic border and delivering the same intensity as the latter; the heat transfer induced by the two real and imaginary heat bands considered in infinite mediums. The temperature at the point $M(X,z)$ due to an elementary segment dl_i of the primary heat source located at the R_1 distance and to another elementary segment dl_i of the image heat source located at the R_2 distance is given according to

$$T_M = \frac{q_{pl}}{2\pi\lambda} \int_{l_i=0}^{L} \exp\Big(-(X - l_i \sin\varphi)\frac{V}{2a}\Big)\Big[K_0\Big(R_1\frac{V}{2a}\Big) + K_0\Big(R_2\frac{V}{2a}\Big)\Big]\, dl_i \tag{2.2}$$

where

$$R_1 = \sqrt{(X - l_i\sin\varphi)^2 + (z - l_i\cos\varphi)^2} \qquad R_2 = \sqrt{(X - l_i\sin\varphi)^2 + (z + l_i\cos\varphi)^2}$$

The heat liberation intensity of the shear band heat source q_{pl} is calculated using the classical orthogonal metal cutting theory (see Appendix A for details) indicated by Hou and Komanduri (1997).

The expressions for V and φ depend on the thermal influence of the primary shear zone in the workpiece and the chip; namely:

- for the workpiece: $V = V_c$ and $\varphi = -(90^\circ + \phi)$
- for the chip: $V = V_{ch}$ and $\varphi = -(\phi - \alpha)$

2.2. Secondary shear zone

Komanduri and Hou (2001a) considered, in the secondary shear zone, the chip as a semi-infinite medium. The heat source having width L moves at the speed of the chip V_{ch} on the border of the medium; the remainder of the border is adiabatic. An image source of the heat source at tool-chip the interface is added to take account of the low thickness t_{ch} of the chip. Figure 3a illustrates the model for thermal analysis of the chip. By adopting the same reasoning of the primary shear zone, the temperature of each point of the medium can be expressed by

$$T_M = \frac{q_{pl}}{\pi\lambda} \int_{l_i=0}^{L} B_{i,chip} \exp\Big(-(X - l_i)\frac{V_{ch}}{2a}\Big)\Big[K_0\Big(\frac{R_i V_{ch}}{2a}\Big) + K_0\Big(\frac{R_i' V_{ch}}{2a}\Big)\Big]\, dl_i \tag{2.3}$$

where

$$R_i = \sqrt{(X - l_i)^2 + z^2} \qquad R_i' = \sqrt{(X - l_i)^2 + (2t_{ch} - z)^2}$$
$$B_{i,chip} = (B_{chip} - \Delta B) + 2\Delta B\Big(\frac{l_i}{L}\Big)^m + C\Delta B\Big(\frac{l_i}{L}\Big)^k$$

Figure 3b illustrates the model for thermal analysis of the tool. The heat source is considered stationary rectangular. The temperature of an unspecified point $M(X, y, z)$ of the tool is given by

$$T_M = \frac{q_{pl}}{2\lambda\pi}\Big[\int_{y_i=-b_0}^{+b_0}\int_{x_i=0}^{L} B_{i,tool}\Big(\frac{1}{R_i} + \frac{1}{R_i'}\Big)\, dx_i\, y_i\Big] \tag{2.4}$$

where

$$R_i = \sqrt{(X - x_i)^2 + (y - y_i)^2 + z^2} \qquad R_i' = \sqrt{(X - 2L + x_i)^2 + (y - y_i)^2 + z^2}$$
$$B_{i,tool} = (B_{tool} + \Delta B) - 2\Delta B\Big(\frac{l_i}{L}\Big)^m - C\Delta B\Big(\frac{l_i}{L}\Big)^k$$

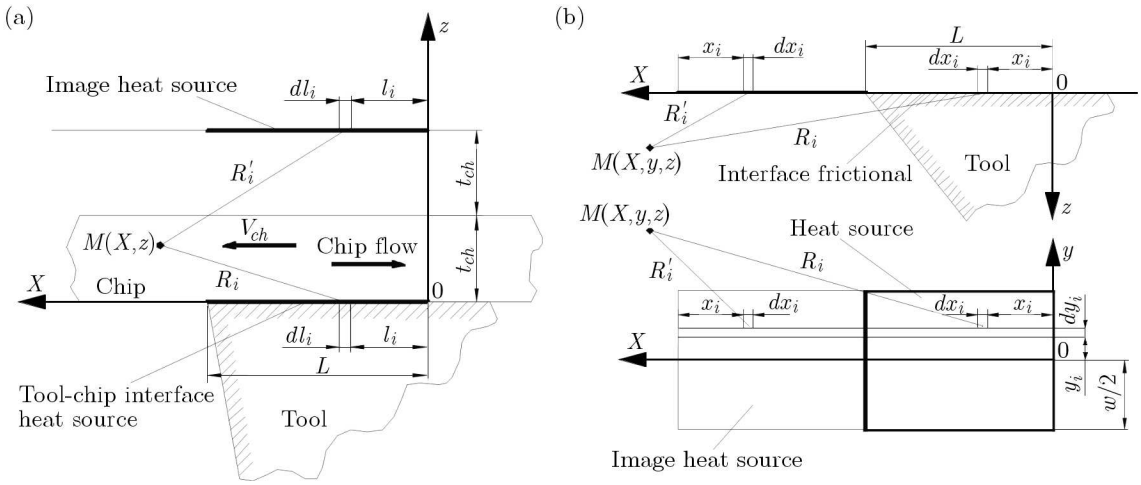

Fig. 3. Heat transfer model for the frictional heat source at the tool-chip interface, (a) on the chip side as a moving band heat source, (b) on the tool as a stationary rectangular heat source

2.3. Combined heating effects of the shearing zones

Komanduri and Hou (2001b) dealt with the temperature rise distribution in metal cutting due to a combined effect of the shear plane heat source in the primary shear zone and the frictional heat source at the tool-chip interface.

Figure 4 shows the sites of the real and imaginary heat sources of the two shearing zones in the chip.

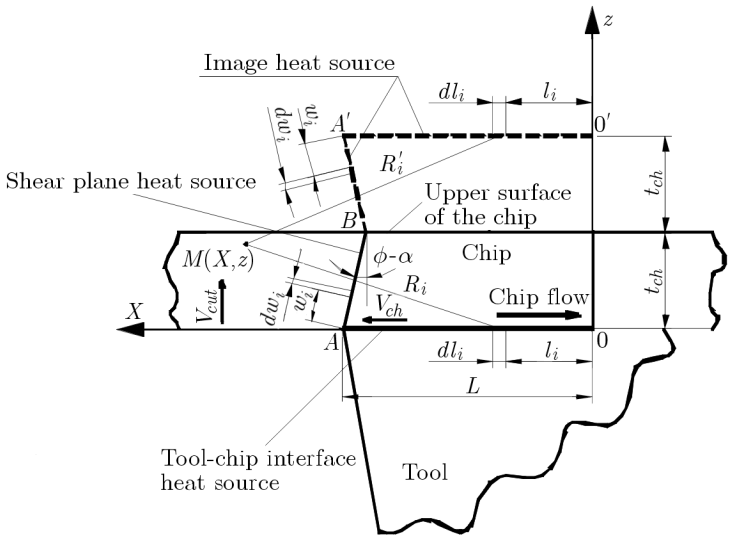

Fig. 4. Common coordinate system for the combined effect of the two principal heat sources

To evaluate temperature at any point $M(X,z)$ of the chip, it is enough to sum the effects of the two heat sources, which gives the following general equation

$$\begin{aligned} T_M = {} & \frac{q_{pl}}{\pi\lambda} \int\limits_{li=0}^{L} \Big[B_{chip} - \Delta B + 2\Delta B\Big(\frac{l_i}{L}\Big)^m + C\Delta B\Big(\frac{l_i}{L}\Big)^k\Big] \exp\Big(\frac{-(X-l_i)V_{ch}}{2a}\Big) \\ & \cdot \Big[K_0\Big(R_i\frac{V_{ch}}{2a}\Big) + K_0\Big(R_i'\frac{V_{ch}}{2a}\Big)\Big]\, dl_i + \frac{q_{pls}}{2\pi\lambda} \int\limits_{w_i=0}^{\frac{t_{ch}}{\cos(\phi-\alpha)}} \exp\Big(\frac{-(X-X_i)V_{ch}}{2a}\Big) \\ & \cdot \Big[K_0\Big(\frac{V_{ch}}{2a}\sqrt{(X-X_i)^2+(z-z_i)^2}\Big) + K_0\Big(\frac{V_{ch}}{2a}\sqrt{(X-X_i)^2+(2t_{ch}-z-z_i)^2}\Big)\Big]\, dw_i \end{aligned} \tag{2.5}$$

where

$$X_i = L - w_i\sin(\phi-\alpha) \qquad z_i = w_i\cos(\phi-\alpha)$$

In the same way for the tool, the temperature at any point $M(X,z)$ caused by the two heat sources is in form of

$$\begin{aligned} T_M = {} & \frac{q_{pl}}{2\pi\lambda_{tool}} \int\limits_{y_i=\frac{-w}{2}}^{+\frac{w}{2}} \int\limits_{x_i=0}^{L} \Big[B_{tool} + \Delta B - 2\Delta B\Big(\frac{x_i}{L}\Big)^m - C\Delta B\Big(\frac{x_i}{L}\Big)^k\Big]\Big(\frac{1}{R_i} + \frac{n}{R_i'}\Big)\, dx_i\, dy_i \\ & + \frac{q_{pli}}{2\pi\lambda_{tool}} \int\limits_{y_i=\frac{-w}{2}}^{+\frac{w}{2}} \int\limits_{x_i=0}^{L} \Big[B_{ind} + \Delta B_i - 2\Delta B_i\Big(\frac{x_i}{L}\Big)^{m_i} - C_i\Delta B_i\Big(\frac{x_i}{L}\Big)^{k_i}\Big]\Big(\frac{1}{R_i} + \frac{n}{R_i'}\Big)\, dx_i\, dy_i \end{aligned} \tag{2.6}$$

where

$$R_i = \sqrt{(X-x_i)^2+(y-y_i)^2+z^2}$$
$$R_i' = \sqrt{(X-2L+x_i)^2+(y-y_i)^2+z^2} \qquad x_i = l_i$$

and q_{pli} is the average heat liberation intensity of the induced heat source [J/cm^{2}s], m_i, k_i, C_i and ΔB are relevant exponents and constants for the induced heat source.

3. Developed model

Komanduri and Hou combined the heat source effects associated with the primary and secondary shear zone for a global prediction of temperature at the tool-chip-workpiece interface. The temperature map obtained is in fact only one superposition of various temperature maps obtained each time one in its own system of axes. Figure 5a shows the system of axes used by Komanduri and Hou (2000, 2001b).

In the present study, we rewrite the equations which express the temperature of the chip, the tool and the workpiece in the same system of axes. For this purpose, the system of axes retained is that of the workpiece shown in Fig. 5b; the mathematical transformations (translation and rotation) carried out can be summarized as follows:

- adapting the system of axes for the temperature map of the chip induced by the heat source of the primary shear zone to the system of axes for the temperature map of the workpiece;
- adapting the system of axes for the temperature map of the chip and the tool due to the heat source of the secondary shear zone to the system of axes for the temperature of the work piece.

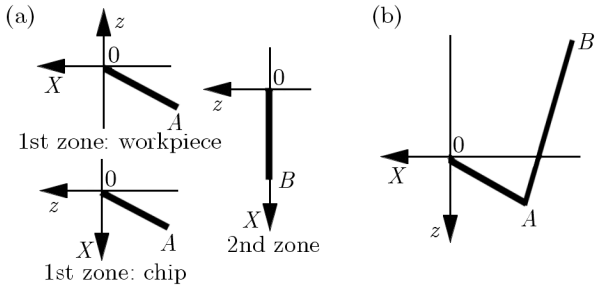

Fig. 5. System of axes (a) used by Komanduri and Hou, (b) retained system of axes

After formula development, we obtain the following general model (Fig. 6).

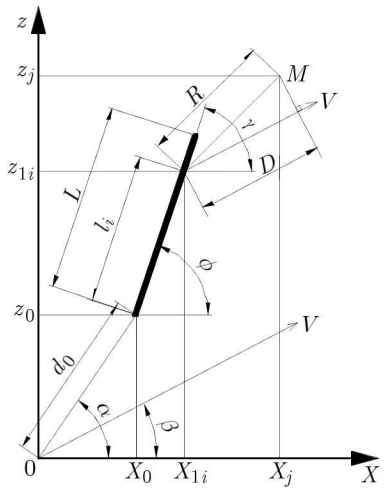

Fig. 6. The general mofel developed by Komanduri and Hou

Considering the general case of a moving heat source with intensity q_i which moves with velocity V, the equation of temperature generated by this source is in the form

$$T_M = \frac{q_i}{2\pi\lambda} \int_0^L \exp\Big(-\frac{V}{2a}D\Big) K_0\Big(\frac{V}{2a}R\Big)\, dl_i \tag{3.1}$$

where R is the distance between M and l_i, D is the projection of R on the line speed V and

$$R = \sqrt{(X_i - X_{li})^2 + (z_j - z_{li})^2}$$
$$X_{li} = X_0 + l_i \cos\phi \qquad z_{li} = z_0 + l_i \sin\phi \qquad X_0 = d_0 \cos\alpha \qquad z_0 = d_0 \sin\alpha$$
$$R = \sqrt{(X_i - d_0\cos\alpha - l_i\cos\phi)^2 + (z_j - d_0\sin\alpha - l_i\sin\phi)^2}$$
$$D = R\cos(\gamma - \beta)$$
$$\cos\gamma = \frac{X_i - X_{li}}{R} = \frac{X_i - d_0\cos\alpha - l_i\cos\phi}{R} \qquad \sin\gamma = \frac{z_j - z_{li}}{R} = \frac{z_j - d_0\sin\alpha - l_i\sin\phi}{R}$$
$$D = \cos\beta(X_i - d_0\cos\alpha - l_i\cos\phi) + \sin\beta(z_j - d_0\sin\alpha - l_i\sin\phi)$$

The equations of the developed models which follow show the effect of each heat source separately in the various zones: tool, chip and workpiece. The temperature at the interface is obtained by summing the effects of the two heat sources.

Temperature equations for the workpiece

- The primary shear zone effect

$$T_M = \frac{q_{pl}}{2\pi\lambda} \int_{l_i=0}^{L} \exp\Big(-(X + l_i\cos\phi)\frac{V_c}{2a}\Big)\Big[K_0\Big(\frac{R_i}{V_c}2a\Big) + K_0\Big(\frac{R_i' V_c}{2a}\Big)\Big]\, dl_i \tag{3.2}$$

where

$$R_i = \sqrt{(X + l_i\cos\phi)^2 + (z - l_i\sin\phi)^2} \qquad R_i' = \sqrt{(X + l_i\cos\phi)^2 + (z + l_i\sin\phi)^2}$$

- The Secondary shear zone effect

$$T_M = \frac{q_{pl}}{\pi\lambda} \int_{l_i=0}^{L} \exp\Big(-(X + L\cos\phi + (L - l_i)\sin\alpha)\frac{V_c}{2a}\Big)\Big[K_0\Big(\frac{R_i V_c}{2a}\Big) + K_0\Big(\frac{R_i' V_c}{2a}\Big)\Big]\, dl_i \tag{3.3}$$

where

$$R_i = \sqrt{[X + L\cos\phi + (L - l_i)\sin\alpha]^2 + [z - L\sin\phi + (L - l_i)\cos\alpha]^2}$$
$$R_i' = \sqrt{[X - L\cos\phi + (L - l_i)\sin\alpha]^2 + [z - L\sin\phi + (L - l_i)\cos\alpha]^2}$$

Temperature equations for the chip

- The primary shear zone effect

$$T_M = \frac{q_{pls}}{2\pi\lambda} \int_{l_i=0}^{L} \exp\Big(-[(X + l_i\cos\phi)\sin(\alpha) + (z - l_i\sin\phi)\cos\alpha]\frac{V_{ch}}{2a}\Big) \cdot \Big[K_0\Big(\frac{R_i V_{ch}}{2a}\Big) + K_0\Big(\frac{R_i' V_{ch}}{2a}\Big)\Big]\, dl_i \tag{3.4}$$

where

$$R_i = \sqrt{(X + l_i\cos\phi)^2 + (z - l_i\sin\phi)^2}$$
$$R_i' = \sqrt{[X + l_i\sin(\phi + 2\alpha)]^2 + [z - l_i\cos(\phi - 2\alpha)]^2}$$

- The secondary shear zone effect

$$T_M = \frac{q_{pl}}{\pi\lambda}\int\limits_{l_i=0}^{L}\Big[B_{chip} - \Delta B + 2\Delta B\Big(\frac{l_i}{L}\Big)^m + C\Delta B\Big(\frac{l_i}{L}\Big)^k\Big] \cdot \exp\Big(-(z - L\sin\phi) + (L - l_i)\cos\alpha\frac{V_{ch}}{2a}\Big)\Big[K_0\Big(\frac{R_i V_{ch}}{2a}\Big) + K_0\Big(\frac{R_i' V_{ch}}{2a}\Big)\Big]\, dl_i \tag{3.5}$$

where

$$R_i = \sqrt{(X + l_i\cos\phi)^2 + (z - l_i\sin\phi)^2}$$
$$R_i' = \sqrt{[X + l_i\cos(\phi + 2\alpha)]^2 + (z - l_i\sin(\phi - 2\alpha)]^2}$$

Temperature equations for the tool

- The primary shear zone effect

$$T_M = \frac{q_{pli}}{2\pi\lambda_{tool}}\int\limits_{y_i=\frac{-w}{2}}^{\frac{+w}{2}}\int\limits_{l_i=0}^{L}\Big[B_i + \Delta B_i - 2\Delta B_i\Big(\frac{l_i}{L}\Big)^{m_i} - C\Delta B_i\Big(\frac{l_i}{L}\Big)^{k_i}\Big]\Big(\frac{1}{R_i} + \frac{n}{R_i'}\Big)\, dl_i \tag{3.6}$$

where

$$R_i = \sqrt{[X + L\cos\phi + (L - l_i)\sin\alpha]^2 + [z - L\sin\phi + (L - l_i)\cos\alpha]^2 + \Big(\frac{w}{2} - y_i\Big)^2}$$
$$R_i' = \sqrt{[X + L\cos\phi - (L - l_i)\sin\alpha]^2 + [z - L\sin\phi - (L - l_i)\cos\alpha]^2 + \Big(\frac{w}{2} - y_i\Big)^2}$$

- The secondary shear zone effect

$$T_M = \frac{q_{pl}}{2\pi\lambda_{tool}}\int\limits_{y_i=\frac{-w}{2}}^{\frac{+w}{2}}\int\limits_{l_i=0}^{L}\Big[B_{tool} + \Delta B - 2\Delta B\Big(\frac{l_i}{L}\Big)^m - C\Delta B\Big(\frac{l_i}{L}\Big)^k\Big]\Big(\frac{1}{R_i} + \frac{n}{R_i'}\Big)\, dl_i \tag{3.7}$$

where

$$R_i = \sqrt{[X + L\cos\phi + (L - l_i)\sin\alpha]^2 + [z - L\sin\phi + (L - l_i)\cos\alpha]^2 + \Big(\frac{w}{2} - y_i\Big)^2}$$
$$R_i' = \sqrt{[X + L\cos\phi - (L - l_i)\sin\alpha]^2 + [z - L\sin\phi - (L - l_i)\cos\alpha]^2 + \Big(\frac{w}{2} - y_i\Big)^2}$$

3.1. Simulation of the developed model

Now we carry out a simulation of the developed model. First of all, we will expose the results relating to the temperature distributions in the workpiece and the chip due to the heat source of the primary shear zone, thereafter we group these two temperature maps. Then, we present the temperature distributions in the tool and the chip due to the heat source of the secondary shear zone. Finally, we combine the heat effects associated with the primary and secondary shear zones for a global prediction of temperature in the tool-chip-workpiece interface.

In order to reduce the computing time, we proposed the flow chart which expresses the programs for the temperature distributions determination in the tool-chip-workpiece interface in the same system of axes which is schematized in Fig. 7. Let us note that for future comparison with the reference by Komanduri and Hou (2001a,b), our simulations were carried out with the same simulation parameters:

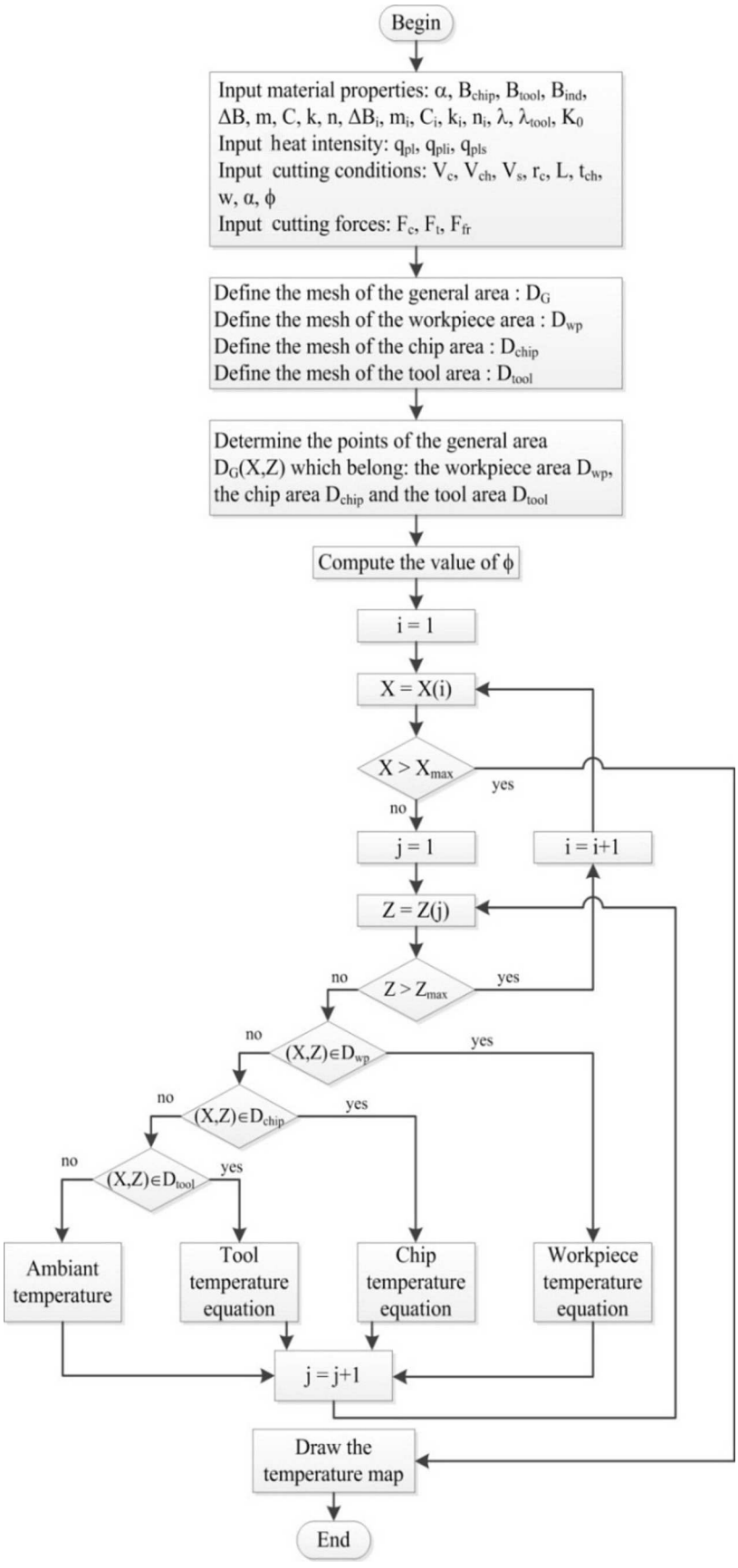

Fig. 7. Flow chart of the determination of the temperature map for the developed model

- Work material: NE 9445 steel, Tool: Carbide
  - material properties: $B_{chip} = 0.620$, $B_{tool} = 0.380$, $B_{ind} = 1$, $\Delta B = 0.35$, $m = 0.24$, $C = 2$, $k = 16$, $n = 1$, $\Delta B_i = 0.8$, $m_i = 0.3$, $C_i = 0.2$, $K_i = 4$, $n_i = 1$, $\lambda = 0.3888\,\mathrm{w/cm^\circ C}$, $\lambda_{tool} = 0.4190\,\mathrm{w/cm^\circ C}$;
  - cutting conditions: $V_c = 152.4\,\mathrm{cm/s}$, $V_{ch} = 57.15\,\mathrm{cm/s}$, $V_s = 158, 98\,\mathrm{cm/s}$, $r_c = 0.375$, $L = 0.1209\,\mathrm{cm}$, $t_{ch} = 0.06637\,\mathrm{cm}$, $w = 0.2591\,\mathrm{cm}$, $\alpha = 4^\circ$, $\phi = 21.01^\circ$;
  - cutting forces: $F_C = 1681.3\,\mathrm{N}$, $F_t = 854.0\,\mathrm{N}$, $F_{fr} = 969.2\,\mathrm{N}$;
  - heat intensity: q_{pl}, q_{pli} and q_{pls}.
- Heat liberation rate of the frictional heat source per unit area: $q_{pl} = F_{fr}v_{ch}/(100Lw) = 17682.2\,\mathrm{J/cm^2s}$.
- Shear plane length: $\overline{AB} = t_{ch}/\cos(\phi - \alpha) = 0.06942$.
- Total heat liberation rate of the shear plane heat source q_s: $q_s = F_c v_c/100 - F_{fr}v_{ch}/100 = 2008.4\,\mathrm{J/s}$.
- Heat liberation rate of the shear plane heat source per unit area: $q_{pls} = q_s/(\overline{AB}w) = 111660\,\mathrm{J/cm^2}$.
- $q_{pli} = 1800\,\mathrm{J/cm^2s}$ is the average heat liberation intensity of the induced heat source. It is constant for the induced heat source.

In the following section, we will present the temperature map.

3.2. Temperature distributions in the workpiece and the chip due to the primary shear zone

The developed model of Komanduri and Hou for the primary shear zone was simulated for machining conditions indicated in the reference by Komanduri and Hou (2000).

The temperature maps (Figs. 8, 9 and 10) show respectively the temperature distributions in the workpiece and the chip as well as the combination of the two temperature maps in the same system of axes due to the heat source effect in the primary shear zone.

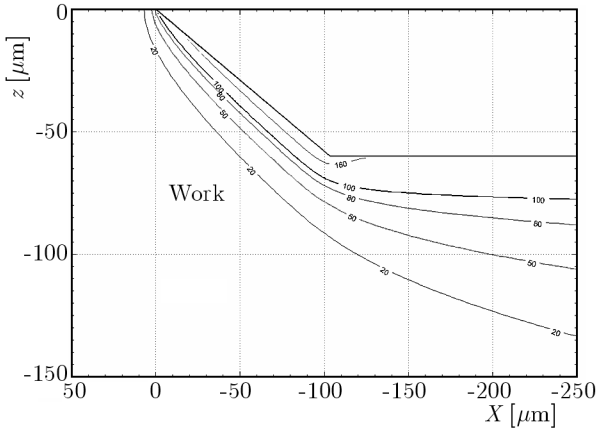

Fig. 8. Temperature distributions in the workpiece due to the heat source effect of in the primary shear zone

3.3. Temperature distributions in the chip and the tool due to the secondary shear zone

The developed model of Komanduri and Hou for the secondary shear zone was simulated for the conditions of machining indicated in the reference by Komanduri and Hou (2001a).

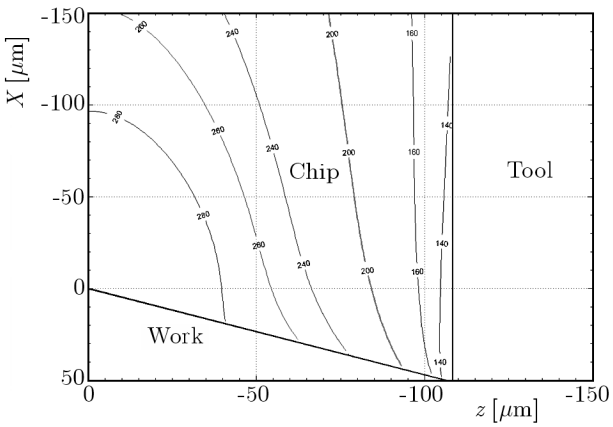

Fig. 9. Temperature distributions in the chip due to the heat source effect in the primary shear zone

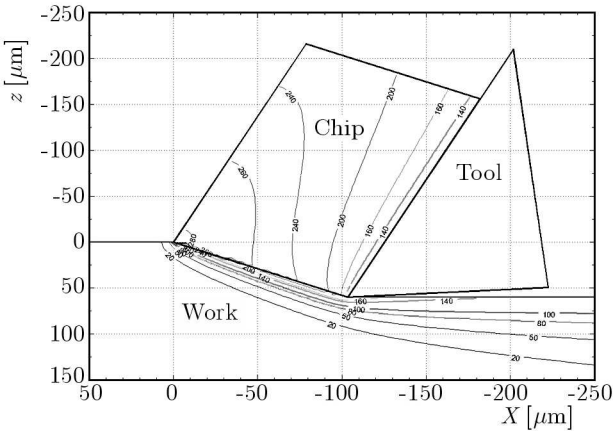

Fig. 10. Temperature distributions in the workpiece and the chip due to the heat source effect in the primary shear zone

The temperature map (Fig. 11) shows the temperature distributions in the chip and the tool due to the heat source effect in the secondary shear zone.

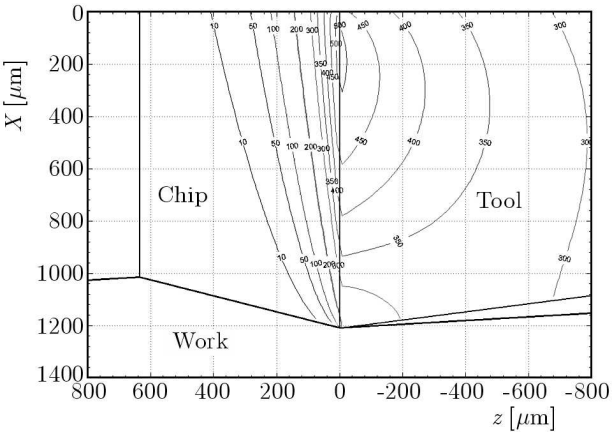

Fig. 11. Temperature distributions in the tool and the chip due to the heat source effect in the secondary shear zone

3.4. Temperature distributions due to the combined heat sources effect of the shear zones

The developed model of Komanduri-Hou for the heat sources effect in the primary and secondary shears zones was simulated for machining conditions indicated in the reference by Komanduri and Hou (2001b).

The temperature maps (Figs. 12, 13 and 14) show respectively the temperature distributions in the tool-chip-workpiece interface due to the individual and combined heat sources effects of in the primary and secondary shear zones. Our simulation results compared to the original maps showed a perfect correspondence.

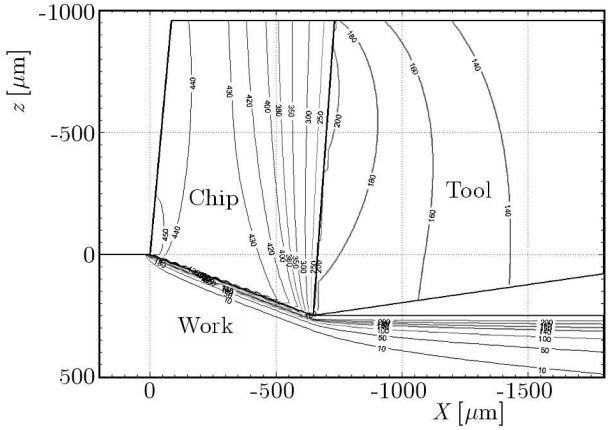

Fig. 12. The heat source effect in the primary zone

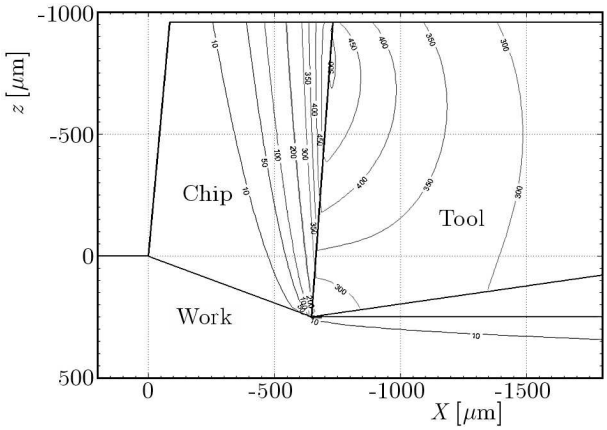

Fig. 13. The heat source effect in the secondary zone

The various temperature maps, confronted with those provided by the developments of Komanduri and Hou (2000, 2001a,b), seem very promising.

4. Conclusion

In this study, we developed a thermal model of Komanduri and Hou, then proceeded to simulations. The modifications we brought can be inserted in adaptive control applications of the machining process.

For this purpose, we carried out mathematical transformations on the original model to predict temperature maps in the tool-chip interface.

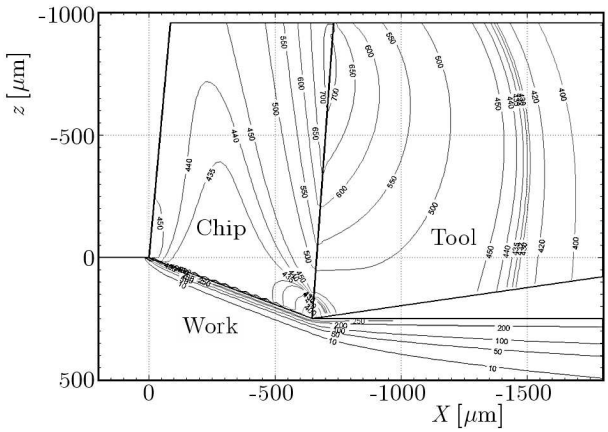

Fig. 14. Combined effects of the heat sources

The results obtained are very promising for temperature distribution predictions, expressed in maps in form of isotherms. The temperature is therefore quantified in regions formed by the workpiece, the tool and the chip.

References

1. Blok H., 1938, Theoretical study of temperature rise at surface of actual contact under oiliness lubricating conditions, *Proceedings of General Discussion on Lubrication and Lubricants*, Institution of Mechanical Engineers, 222-235
2. Boothroyd G., 1963, Temperatures in orthogonal metal cutting , *Pro Institution of the Mechanical Engineers*, G.I. London, **177**, 29, 789-810
3. Chao B.T., Trigger K.J., 1953, The significance of the thermal number in metal cutting, *ASME Transactions of American Society of Mechanical Engineers*, **75**, 109-120
4. Chao B.T., Trigger K.J., 1955, Temperature distribution at the tool-chip interface in metal cutting, *ASME Transactions of American Society of Mechanical Engineers*, **77**, 2, 1107-1121
5. Chao B.T., Trigger K.J., 1958, Temperature distribution at tool-chip and tool-work interface in metal cutting, *ASME Transactions of American Society of Mechanical Engineers*, **20**, 1, 311-320
6. Carslaw H.S., Jaeger J.C., 1959, *Conduction of Heat in Solids*, Oxford, UK, Oxford University Press
7. Jaeger J.C., 1942, Moving sources of heat and the temperatures at sliding contacts, *Proceedings Royal Society of NSW*, **76**, 203-224
8. Hahn R.S., 1951, On the temperature developed at the shear plane in the metal cutting process, *Proceedings of First US National Congress of Applied Mechanics*, 661-666
9. Huang Y., Liang S. Y., 2005, Cutting temperature modeling based on non-uniform heat intensity and partition ratio, *Machining Science and Technology*, **9**, 301-323
10. Karpat Y., Özel T., 2006, Predictive analytical and thermal modeling of orthogonal cutting process – Part I: Predictions of tool forces, stresses, and temperature distributions, *ASME Transactions of American Society of Mechanical Engineers*, **128**, 435-444
11. Karpat Y., Özel T., 2008, Analytical and thermal modeling of high-speed machining with chamfered tools, *ASME Transactions of American Society of Mechanical Engineers*, **130**, 0110014-01--011001-15
12. Hou Z.B., Komanduri R., 1997, Modeling of thermomechanical shear instability in machining, *International Journal of Mechanical Sciences*, **39**, 11, 1273-1314

13. Komanduri R., Hou Z.B., 2000, Thermal modeling of the metal cutting process, Part I: Temperature rise distribution due to shear plane heat source, *International Journal of Mechanical Sciences*, **42**, 1715-1752

14. Komanduri R., Hou Z.B., 2001a, Thermal modeling of the metal cutting process, Part II: Temperature rise distribution due to frictional heat source at the tool-chip interface, *International Journal of Mechanical Sciences*, **43**, 57-88

15. Komanduri R., Hou Z.B., 2001b, Thermal modeling of the metal cutting process, Part III: Temperature rise distribution due to the combined effects of shear plane heat source and the tool-chip interface frictional heat source, *International Journal of Mechanical Sciences*, **43**, 89-107

16. Loene W.C., 1954, Distribution of shear-zone heat in metal cutting, *ASME Transactions of American Society of Mechanical Engineers*, **76**, 121-125

17. Loewen E.G., Shaw M.C., 1954, On the analysis of cutting tool temperatures, *ASME Transactions of American Society of Mechanical Engineers*, **76**, 217-231

18. Rosenthal D., 1946, The theory of moving sources of heat and its application to metal treatments, *ASME Transactions of American Society of Mechanical Engineers*, **68**, 849-866

19. Trigger K.J., Chao B.T., 1951, An analytical evaluation of metal cutting temperature, *ASME Transactions of American Society of Mechanical Engineers*, **73**, 57-68

20. Wright P.K., McCormic, S.P., Miller T. R., 1980, Effect of rake face design on cutting tool temperature distributions, *ASME Journal of Engineering for Industry*, **102**, 2, 123-128

Manuscript received June 18, 2012; accepted for print September 17, 2012